Research Article

INTERNATIONAL JOURNAL OF ADVANCED ROBOTIC SYSTEMS

International Journal of Advanced Robotic Systems
September-October 2017: 1–10
© The Author(s) 2017
DOI: 10.1177/1729881417733934
journals.sagepub.com/home/arx
SAGE

A new redundancy resolution for underwater vehicle–manipulator system considering payload

Yaoyao Wang[1,2], Surong Jiang[1], Fei Yan[1], Linyi Gu[2] and Bai Chen[1]

Abstract

For the motion coordination problem between the underwater vehicle and manipulator of the underwater vehicle–manipulator system, a new redundancy resolution method is proposed and investigated. The proposed method mainly has two parts: a fuzzy logic part and a multitasks weighted gradient projection method part. The fuzzy logic part is used to decide the weight factors of the motion distribute matrix and the priorities of all the secondary objectives, while the multitasks weighted gradient projection method part is used to handle the secondary objectives with the weight factors and priorities decided by the fuzzy logic part. Moreover, a new secondary objective is proposed to optimize underwater vehicle–manipulator system's attitude, which takes the payload into consideration. Finally, the effectiveness of the proposed redundancy resolution is verified through some comparative simulations.

Keywords

Motion coordination, underwater vehicle–manipulator system (UVMS), redundancy resolution, payload

Date received: 18 June 2017; accepted: 5 August 2017

Topic: Mobile Robots and Multi-Robot Systems
Topic Editor: Nak-Young Chong
Associate Editor: Genci Capi

Introduction

In recent few decades, underwater vehicle–manipulator systems (UVMS) have been widely used in the underwater working applications due to their good capabilities in the deep ocean, especially the area where human driver can hardly arrive.[1–3] Generally speaking, the UVMS consists of an underwater vehicle and one or more manipulators. However, the most popular type of UVMS nowadays is still the remotely operated vehicle–manipulator system (ROVMS), which means at least one human pilot is required. Usually, the ROV and corresponding manipulator are controlled separately by the pilot during the tasks, or the ROV keeps station automatically while only the manipulator is manually controlled. This operation mode is simple but sometimes inefficient because the inherent redundancy of UVMS is totally eliminated.

To solve the abovementioned problem and improve the working efficient of UVMS, the position and orientation of UVMS's end-effector can be directly commanded to perform the tasks. This operation mode can effectively exploit the redundancy of UVMS and lead to more flexible working ability. Therefore, the redundancy resolution problem

[1] College of Mechanical and Electrical Engineering, Nanjing University of Aeronautics and Astronautics, Nanjing, China
[2] The State Key Laboratory of Fluid Power Transmission and Control, Zhejiang University, Hangzhou, China

Corresponding author:
Bai Chen, College of Mechanical and Electrical Engineering, Nanjing University of Aeronautics and Astronautics, Yudao Road 29, Nanjing, Jiangsu 210016, China.
Email: chenbye@126.com

had been widely studied to properly adopt the abovementioned mode since the UVMS usually has more than six degree of freedoms (DOFs). After the redundancy resolution problem is properly handled, advanced control methods[4–10] can be applied to enhance the working precision.

There are mainly two methods for the redundancy resolution of UVMS, namely pseudoinverse of the Jacobian matrix method and gradient projection method (GPM). The first one, proposed by Whitney in 1969,[11] is focused on the minimum norm solution on the speed level. The later one, proposed by Liegeois in 1977,[12] is developed to utilize the null-space joint speed for the secondary tasks. Since then many redundancy resolutions had been proposed and investigated based on these two methods,[13,14] To avoid both the kinematic and algorithmic singularities with traditional task-priority redundancy resolution for the manipulators, the singularity-robust algorithm was merged with task-priority redundancy resolution.[15] Afterward, a task-priority redundancy resolution was specially proposed for the UVMS based on this method. To handle the different dynamic characteristic of underwater vehicle and manipulator, two novel fuzzy logic (FL)-based task priority redundancy resolutions were proposed.[16,17] The FL was adopted to properly distribute the motion between the underwater vehicle and manipulator and calculate the weight coefficients for all the secondary tasks. To minimize the hydrodynamic force/moment acting on the UVMS, a new redundancy resolution for the UVMS was given and investigated.[18] The method was constructed on the acceleration level to conveniently combine the dynamic controller. A novel FL-based fault-tolerant redundancy resolution was proposed and investigated for the UVMS to handle the fault joints of the manipulator.[19] To reduce the required force/moment during a task, a novel redundancy resolution based on the generalized velocity components was proposed and investigated.[20]

Exciting results had been obtained nowadays concerning the redundancy resolution for UVMS. However, few works had taken the payload into consideration. The attitude of UVMS can be greatly affected if the payload is relatively large and no proper redundancy resolution is adopted. To solve this problem, a novel redundancy resolution using a new designed secondary objective is proposed and investigated in this article. The proposed method combines the FL with multitasks weighted GPM and can effectively ensure the attitude of UVMS stable with the new proposed secondary objective.

The contributions we try to make in this article are to

1. give a new UVMS attitude optimization index design, which takes the payload into consideration;
2. propose a new multitasks weighted GPM with FL using the newly given index and verify its effectiveness through three comparative simulations.

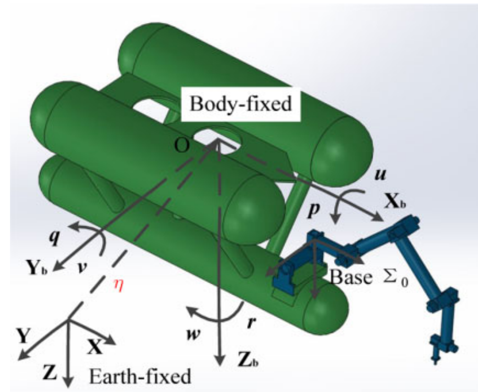

Figure 1. Definition of the coordinate frames for an UVMS. UVMS: underwater vehicle–manipulator system.

The remainder of this work is organized as follows. In section "Kinematic modeling," the kinematic model of UVMS is briefly introduced. In section "Proposed redundancy resolution," the proposed method is given. In section "Simulation studies," some comparative simulations are performed to verify the effectiveness of our proposed method. Final section concludes this work.

Kinematic modeling

The simplified kinematic model of an UVMS containing a 6-DOFs underwater vehicle and an n-DOFs underwater manipulator for an m-dimensional task, as shown in Figure1, can be expressed as[20]

$$\dot{\varsigma}_e = \begin{bmatrix} {}^i\dot{p}_e \\ {}^i\dot{r}_e \end{bmatrix} = \begin{bmatrix} J_{v1} & -[J_{v1}{}^v p_{v,e}\times]J_{v2} & J_{v1}J_{mp} \\ 0_{3\times3} & J_{v2} & J_{v2}J_{mo} \end{bmatrix} \begin{bmatrix} v_1 \\ v_2 \\ \dot{q} \end{bmatrix} \tag{1}$$

where $\varsigma_e = [{}^ip_e^T \quad {}^ir_e^T]^T$ and $\varsigma_{v,e} = [{}^vp_{v,e}^T, \quad {}^vr_{v,e}^T,]^T$ are used to describe the position and orientation of the end-effector in the inertial fixed frame and vehicle fixed frame, respectively. $\eta = [{}^ip_v^T \quad {}^ir_v^T]^T$, ${}^ip_v = [x \quad y \quad z]^T$, and ${}^ir_v = [\phi \quad \theta \quad \psi]^T$ denote the position and orientation vectors of the underwater vehicle in the inertial fixed frame as shown in Figure 1. $v = [v_1 \quad v_2]^T$, $v_1 = [u \quad v \quad w]^T$, and $v_2 = [p \quad q \quad r]^T$ are corresponding linear and angular velocity vectors. The n-DOF joint angular position of the underwater manipulator is defined as $q = [q_1 \quad q_2 \quad \dots \quad q_n]^T$. J_{v1} and J_{v2} are the linear and angular velocity transformation matrices from the inertial fixed frame to the vehicle fixed frame, which can be expressed as equations (2) and (3), respectively. J_{mp} and J_{mo} stand for the position and orientation Jacobian matrices from the vehicle base to the end-effector, more details refer to Ismail and Dunnigan[20]

$$J_{v1}({}^{i}r_v) = \begin{bmatrix} c\psi c\theta & -s\psi c\phi + c\psi s\theta s\phi & s\psi s\phi + c\psi c\phi s\theta \\ s\psi c\theta & c\psi c\phi + s\phi s\theta s\psi & -c\psi s\phi + s\theta s\psi c\phi \\ -s\theta & c\theta s\phi & c\theta c\phi \end{bmatrix} \tag{2}$$

$$J_{v2}({}^{i}r_v) = \begin{bmatrix} 1 & s\phi t\theta & c\phi t\theta \\ 0 & c\phi & -s\phi \\ 0 & s\phi/c\theta & c\phi/c\theta \end{bmatrix} \tag{3}$$

where s·= sin(·), c·= cos(·), and t·= tan(·). And $[J_{v1}{}^{v}p_{v,e}\times]$ is the skew symmetric matrix, for $J_{v1}{}^{v}p_{v,e} = [a \quad b \quad c]^T$, we have

$$[J_{v1}{}^{v}p_{v,e}\times] = \begin{bmatrix} 0 & -c & b \\ c & 0 & -a \\ -b & a & 0 \end{bmatrix} \tag{4}$$

Equation (1) can be further expressed as

$$\dot{\varsigma}_e = J_{vm}\xi \tag{5}$$

where J_{vm} is the UVMS Jacobian matrix and $\xi = [v_1^T \quad v_2^T \quad \dot{q}^T]^T$.

Proposed redundancy resolution

Redundancy resolution

In this subsection, some redundancy resolutions are reviewed, and then our new redundancy resolution will be proposed in the following subsection. The basic way to obtain a redundancy resolution for the UVMS is to adopt the pseudoinverse of the Jacobian matrix as[21]

$$\xi = J_{vm}^{+}\dot{\varsigma}_e \tag{6}$$

where J_{vm}^{+} is the pseudoinverse of J_{vm} and can be obtained using $J_{vm}^{+} = J_{vm}^T(J_{vm}J_{vm}^T)^{-1}$.

This is a redundancy resolution in the least-square sense aiming to minimize the velocity of UVMS. It treats the underwater vehicle/manipulator equally without any difference, which is not suitable for practical applications since the dynamics characteristic of the vehicle and manipulator is quite different. Usually, the vehicle is much larger and heavier than the manipulator. Moreover, the propellers of vehicle have large time constants, while the joint motors of a manipulator have relatively smaller time constants. All the abovementioned elements will result in quite different dynamics between the vehicle and manipulator: the vehicle is suitable for slow and large amplitude motion, while the manipulator is suitable for fast and small amplitude motion. Furthermore, no other constraints can be handled with this method.

By minimizing a cost function $\xi^T\xi$, a general solution for equation (5) can be obtained as

$$\xi = J_{vm}^{+}\dot{\varsigma}_e + (I - J_{vm}^{+}J_{vm})\chi \tag{7}$$

where $\chi \in R^{6+n}$ is an arbitrary UVMS velocity vector and $(I - J_{vm}^{+}J_{vm})$ is a null-space matrix which projects χ onto the null-space of the Jacobian J_{vm}. Corresponding projection will not result in the movement of the end-effector, but only internal movements within the UVMS are produced.

The widely used GPM is based on the selection of χ which is relative to the gradient of a scalar objective function $H(q)$ as

$$\chi = -\lambda\nabla H(q) \tag{8}$$

Combining equations (7) and (8), the GPM can be expressed as

$$\xi = J_{vm}^{+}\dot{\varsigma}_e - \lambda(I - J_{vm}^{\dagger}J_{vm})\nabla H(q) \tag{9}$$

where λ is a factor. When λ is positive, equation (9) gives the minimization of $H(q)$. Otherwise, equation (9) gives the maximization of $H(q)$.

The multiple objectives version of GPM can be expressed as

$$\xi = J_{vm}^{+}\dot{\varsigma}_e - \lambda(I - J_{vm}^{+}J_{vm})\left(\sum_{i=1}^{k}\alpha_i\nabla h_i(q)\right) \tag{10}$$

where k is the quantity of the kinematic constraints and α_i is the weight factor that decides the importance of the ith kinematic constraint. $\nabla h_i(q)$ is the normalized gradient of $H(q)$ which is used to prevent a certain single kinematic constraint from dominating the whole part of $\sum_{i=1}^{k}\alpha_i\nabla h_i(q)$, it can be expressed as

$$\nabla h_i(q) = \nabla H_i(q)/||\nabla H_i(q)||_2 \tag{11}$$

Moreover, if some particular DOF in UVMS needs to be handled, the above method will fail. In this situation, a weighted pseudoinverse $J_{vm\_w}^{\dagger}$ can be used as

$$J_{vm\_w}^{+} = w^{-1}J_{vm}^T(J_{vm}w^{-1}J_{vm}^T)^{-1} \tag{12}$$

where $w^{-1} = \mathrm{diag}(w_1, w_2, ..., w_{6+n})$ is a weight matrix with positive elements.

Combining equations (3) and (9), we have

$$\xi = w^{-1}J_{vm}^T(J_{vm}w^{-1}J_{vm}^T)^{-1}\dot{\varsigma}_e = J_{vm\_w}^{+}\dot{\varsigma}_e \tag{13}$$

The optimal effect of weighted pseudoinverse method equation (13) is weaker compared with GPM, but it has an attractive nature as the end-effector stops moving, the internal movement of UVMS will vanish. This is very important for precise tracking control.

Motion objectives

In this subsection, some motion objectives are presented and analyzed based on the characteristic of our developed UVMS, shown in Figure 1.

Motion distribution. The underwater vehicle and manipulator are suitable for different tasks due to their different dynamic properties. Underwater manipulator has relatively smaller inertia, faster response, and higher precision. These properties make it suitable for tasks that frequently change over time and only need small range of motion. Underwater vehicle, on the other hand, has relatively larger inertia, slower response, and lower precision, which are, nevertheless, suitable for tasks that slowly change over time and need a wide range of motion. Therefore, it is better to use the underwater manipulator when the targets are in its dexterous work space. This can be realized using the method of weighted pseudoinverse with the motion distribution matrix as[21]

$$w^{-1} = \begin{bmatrix} (1-\beta) w_{\max} I_{6\times 6} & 0_{6\times n} \\ 0_{n\times 6} & \beta I_{n\times n} \end{bmatrix} \tag{14}$$

where $0 \le \beta \le 1$, and it basically decides the motion distribution between underwater vehicle and manipulator. The system is attempted to use underwater manipulator when β is relatively large, otherwise the underwater vehicle will be used. Specially, only underwater vehicle or manipulator will be used when $\beta = 0$ or $\beta = 1$. $w_{\max}$ is a constant parameter used to define the maximum value of the weight factor for the underwater vehicle. It has a range of $0 < w_{\max} \le 1$.

Manipulator joint limitation. Manipulator joint limitation is necessary to avoid collision and damage to the hardware. The abovementioned GPM is used to handle this object, and the corresponding *H*(*q*) can be expressed as[19,22]

$$H(q) = \sum_{i=1}^{n} \frac{(q_{i,\max} - q_{i,\min})^2}{C_i (q_{i,\max} - q_i)(q_i - q_{i,\min})} \tag{15}$$

where q_i is the angular value for the *i*th joint, while $q_{i,\min}$, $q_{i,\max}$ stand for the lower and upper bounds of the displacement, respectively. C_i is a positive constant used to determine the strength of the corresponding constraint. Moreover, the gradient of *H*(*q*) can be calculated as

$$\frac{\partial H(q)}{\partial q_i} = \frac{(q_{i,\max} - q_{i,\min})^2 (2q_i - q_{i,\max} - q_{i,\min})}{C_i (q_{i,\max} - q_i)^2 (q_i - q_{i,\min})^2}, \quad i = 1 \sim n \tag{16}$$

Define the weight matrix as $w^{-1} = \mathrm{diag}(w_1, w_2, \ldots, w_n)$ for the manipulator, the corresponding elements can be selected as

$$w_i = \frac{1}{1 + \left| \frac{\partial H(q)}{\partial q_i} \right|}, \quad i = 1 \sim n \tag{17}$$

According to equations (16) and (17), $w_i = 1$ when the underwater manipulator is in the middle of its motion range. Therefore, we have $w_i \in (0, 1]$.

Manipulator singularity avoidance. When the underwater manipulator is in a singular configuration, the required driven force for some particular joints will increase sharply which may damage corresponding actuators. Thus, the measure of manipulability (MOM) proposed by Yoshikawa[23] will be adopted to quantize the singularity and help to avoid this situation

Table 1. D–H parameters of our underwater manipulator.

	α_{i-1} (°)	a_{i-1}	d_i	θ_i
1	0	0	0	q_1
2	90	$L_1 = 0.172$	$d_1 = 0.068$	q_2
3	0	$L_2 = 0.33$	$d_2 =$ -0.068	q_3
4	0	$L_3 = 0.33$	$d_3 = 0.068$	q_4
5	−90	$L_4 = 0.242$	$d_4 = 0.048$	q_5
6	0	$L_5 = 0.121$	0	0

$$\delta_{\sin} = \sqrt{\det(J_{\sin} J_{\sin}^T)} \tag{18}$$

where $J_{\sin} \in R^{3\times n}$ is the Jacobian matrix for the end-effector, which includes the first three rows of J_{vm} and its last *n* columns. In order to utilize GPM, take a gradient with respect to q_i, we have

$$\nabla H = \frac{\partial \delta}{\partial q_i} = \delta_{\sin} \operatorname{tr}\left(\frac{\partial J_{\sin}}{\partial q_i} J_{\sin}^{+} \right), \quad i = 1 \sim 5 \tag{19}$$

Optimize UVMS's attitude. Since our underwater vehicle has no ability to control the pitch and roll direction, it is better to keep the UVMS stable with small pitch and roll angles. The UVMS itself has been balanced with the manipulator in the original position. However, when the manipulator stretches out with a relatively large payload, the resulting moment will greatly affect the attitude of UVMS. Therefore, the payload should be taken into consideration besides the own weight of the manipulator. The gravity and buoyancy of manipulator and payload are along *z*-axis, so the new proposed objective function $M(q)$ is designed in *x*–*y* plane as

$$M(q) = ({}^0x_E{}^2 + {}^0y_E{}^2) F \tag{20}$$

where *F* stands for the force acting on the end-effector, ${}^0x_E$ and ${}^0y_E$ stand for the location information of end-effector in the base coordinate frame Σ_0 of the manipulator as shown in Figure 1. And to simplify the analysis, the direction of *F* is assumed to be along *z*-axis which is reasonable because it is mainly caused by gravity and buoyancy. Corresponding gradient of the proposed objective function *M*(*q*) is given as

$$\frac{\partial M(q)}{\partial q_i} = 2\,{}^0x_E \frac{\partial\, {}^0x_E}{\partial q_i} F + 2\,{}^0y_E \frac{\partial\, {}^0y_E}{\partial q_i} F, \quad i = 1 \sim n. \tag{21}$$

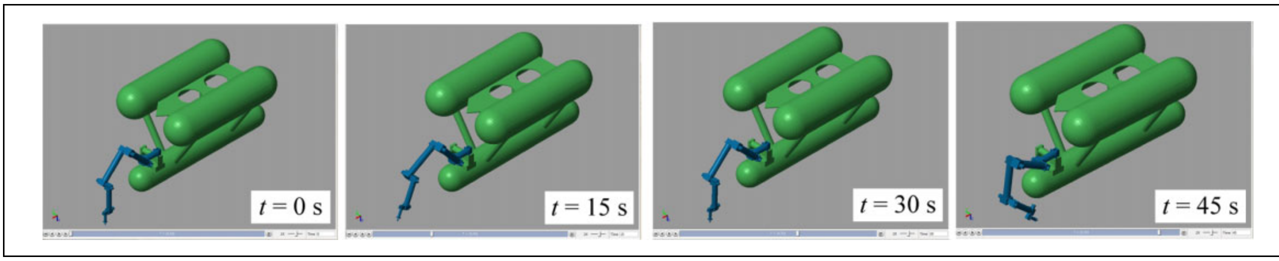

Figure 2. The configuration of the UVMS during case one. UVMS: underwater vehicle–manipulator system.

Remark 1. F can be obtained directly through sensors or indirectly by observer algorithms, but the way to get F will not be taken into consideration in this work.

Proposed redundancy resolution

In order to handle all the abovementioned secondary objectives harmonically, we adopt a multitask weighted GPM–based fuzzy logical algorithm combining equations (7)–(13) as

$$\xi = J^{+}_{vm\_w}(\dot{\varsigma}_{de} + K_e e) + k_H(I_{n\times n} - J^{+}_{vm\_w}J_{vm\_w})\left(\sum_{i=1}^{s}\alpha_i\nabla H_i/||\nabla H_i||_2\right) \tag{22}$$

where $\dot{\varsigma}_{de}$ stands for the desired trajectory of the end-effector. $e = \varsigma_{de} - \varsigma_e$ is the error between the desired and the planned trajectory of the end-effector. K_e is the corresponding gain matrix and s is the number of secondary objectives. Moreover, the fuzzy logical algorithm adopted here mainly has two functions. First, it is used to decide the value of β leading to the motion distribution between the underwater vehicle and manipulator. Second, it is adopted to decide the value of α_i which clearly defines the relative importance among all the secondary objectives.

Simulation studies

In order to illustrate the effectiveness of our proposed redundancy resolution and objective function $M(q)$, comparative numerical simulations have been performed based on the UVMS developed in our laboratory, as shown in Figure 1.

Simulation setup

Our developed UVMS has nine DOFs, four for the underwater vehicle without the ability to control pitch and roll and five for the underwater manipulator. Corresponding Denavit–Hartenberg (D-H) parameters for the underwater manipulator are listed in Table 1. The fuzzy logical algorithm adopted in this work is the same with the one given in the study by Soylu et al.[19], and it is mainly responsible for the manipulator singularity avoidance and UVMS's attitude optimization. Therefore, the final redundancy resolution used in the following simulations is

$$\xi = J^{+}_{vm\_w}(\dot{\varsigma}_{de} + K_e e) + k_H(I_{n\times n} - J^{+}_{w}J_{w})\left(\alpha_1\frac{\nabla H_1}{||\nabla H_1||_2} - \alpha_2\frac{\nabla H_2}{||\nabla H_2||_2}\right) \tag{23}$$

where α_1 is positive and is for manipulator singularity avoidance, α_2 is positive and is for the UVMS's attitude optimization. The negative sign before α_2 means that this GPM part tried to reduce the corresponding objective function. And ∇H_1 is given in equation (19) while ∇H_2 is given in equation (21). The initial position of UVMS is set to $\eta = [0,0,0,0]\mathrm{m}/^{\circ}$, $q = [0,-45,90,45,0]^{\circ}$, and the corresponding position of the end-effector is $x_{\mathrm{E}} = [0.5907,0.053,-0.363]$ expressed in the base coordinate frame Σ_0. The limitation of each joints is set as $q_1 \in [-60, 60]^{\circ}$, $q_2 \in [-90, 90]^{\circ}$, $q_3 \in [-110, 110]^{\circ}$, and $q_{4,5} \in [-120, 120]^{\circ}$. $C_i = [10,6,10,10,10]^{\mathrm{T}}$, $K_e = \mathrm{diag}\{50,50,50\}$, $w_{\max} = 0.02$, and $k_H = 0.2$.

Simulation results

Three cases had been performed. In the first case, the F is set to 0 which means no payload is attached to the manipulator, and the proposed redundancy resolution equation (23) is adopted. In the second case, redundancy resolution equation (6) is adopted. In the third case, the F is set to 50% of the maximum capability of the manipulator, and the proposed redundancy resolution equation (23) is adopted. The end-effector is expected to go forward to the position of 1.2 m along x in 12 s. Then, it will stop for 9 s and go back to the position of -0.5 m with 22 s. Corresponding trajectory will be obtained using the fifth-order polynomial. During this procedure, its position in y- and z-axes remains unchanged.

Corresponding results are given in Figures 2 to 7. As shown in the subfigures (a) and (b) from Figures 3, 5, and 7, the actual trajectories of the end-effector are coincided with the desired ones, which means the end-effector can effectively track the desired trajectory under all three cases.

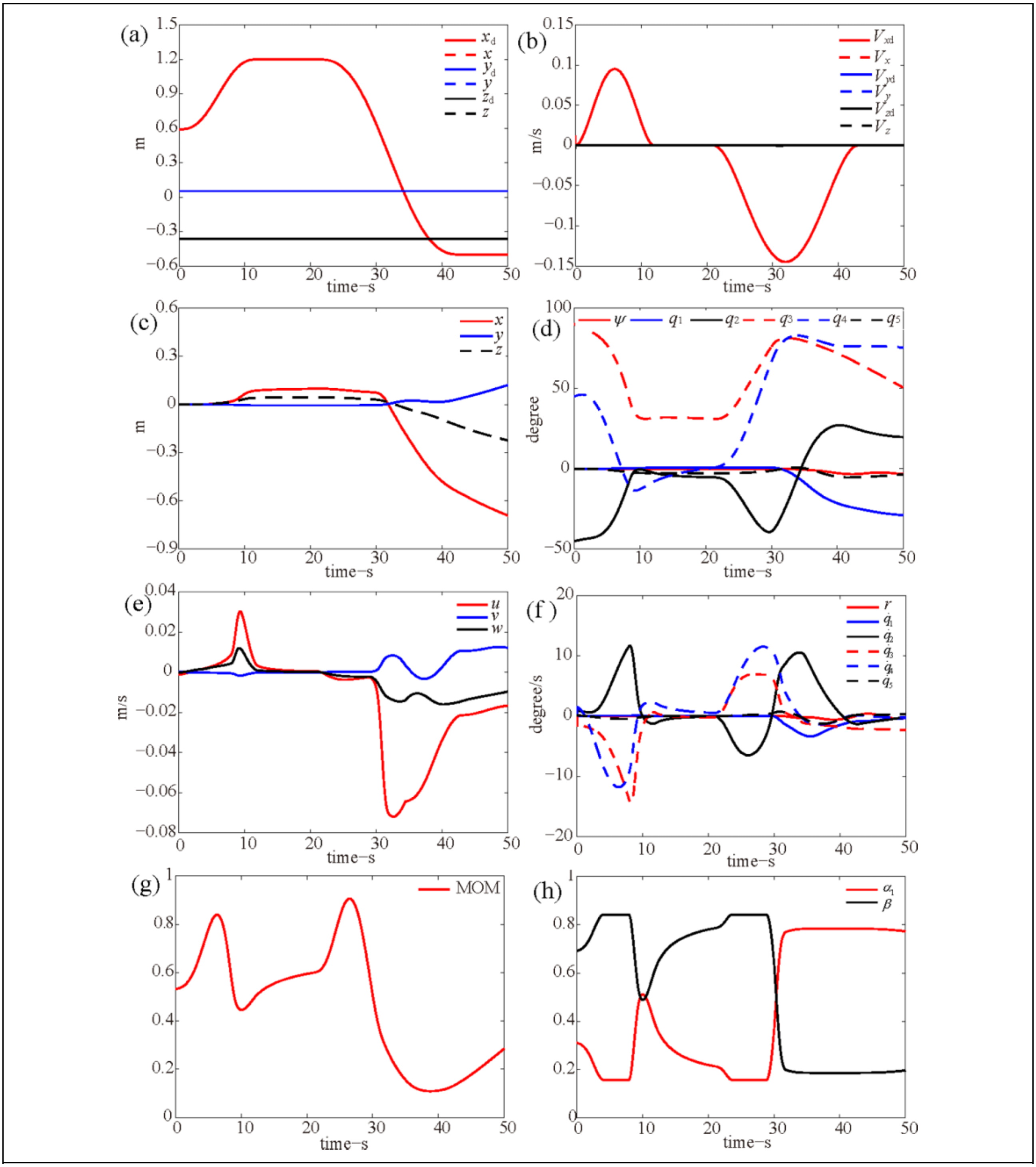

Figure 3. Simulation results under case one. (a) and (b) are the desired trajectory and velocity (solid) versus planned ones (dashed) of the end-effector; (c) and (d) are the planned trajectory for nine DOFs; (e) and (f) are the planned velocity for nine DOFs; (g) is the normalized MOM; and (h) is the output of the fuzzy algorithm α_1, β. DOF: degree of freedom; MOM: measure of manipulability.

Moreover, it can be observed from the simulation results of case one that the underwater vehicle almost keeps still from 0 s to 8 s, this is because in this period, the manipulator is still in its dexterous working space as shown in Figure 3(a) to (d) and (g), therefore, the weight factor β is relatively bigger, while α_1 is relatively smaller as shown in Figure 3(h). Around 10 s, the manipulator moves near its singular configuration, as shown in Figure 3(g), leading to the sharp decrease of MOM. Then, the weight factor β decreases while α_1 increases, leading to the movement of the underwater vehicle. Similar analysis procedure can be used for the left part of the simulation result (Figure 3).

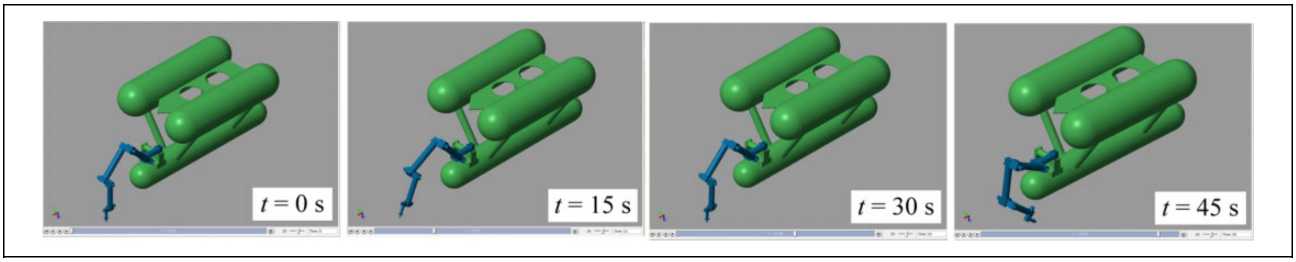

Figure 4. The configuration of the UVMS in a different moment during case two. UVMS: underwater vehicle–manipulator system.

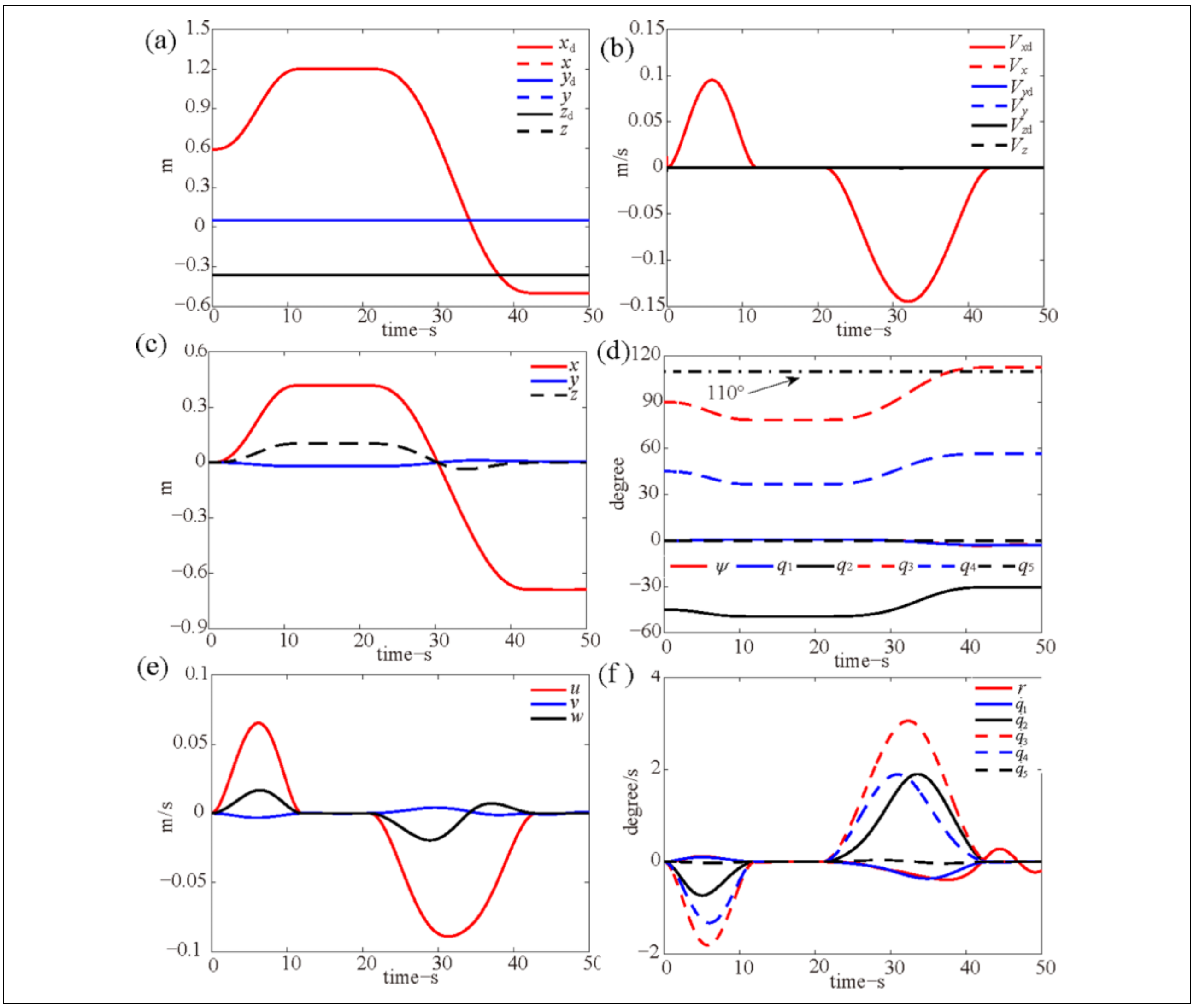

Figure 5. Simulation results under case two. (a) and (b) are the desired trajectory and velocity (solid) versus planned ones (dashed) of the end-effector; (c) and (d) are the planned trajectory for nine DOFs; and (e) and (f) are the planned velocity for nine DOFs. DOF: degree of freedom.

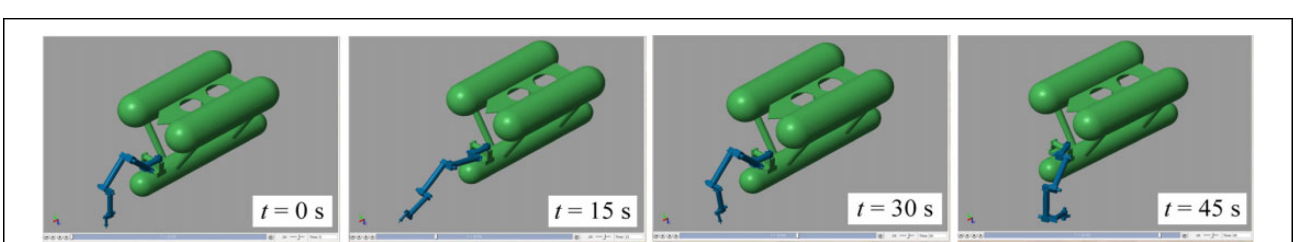

Figure 6. The configuration of the UVMS in a different moment during case three. UVMS: underwater vehicle–manipulator system.

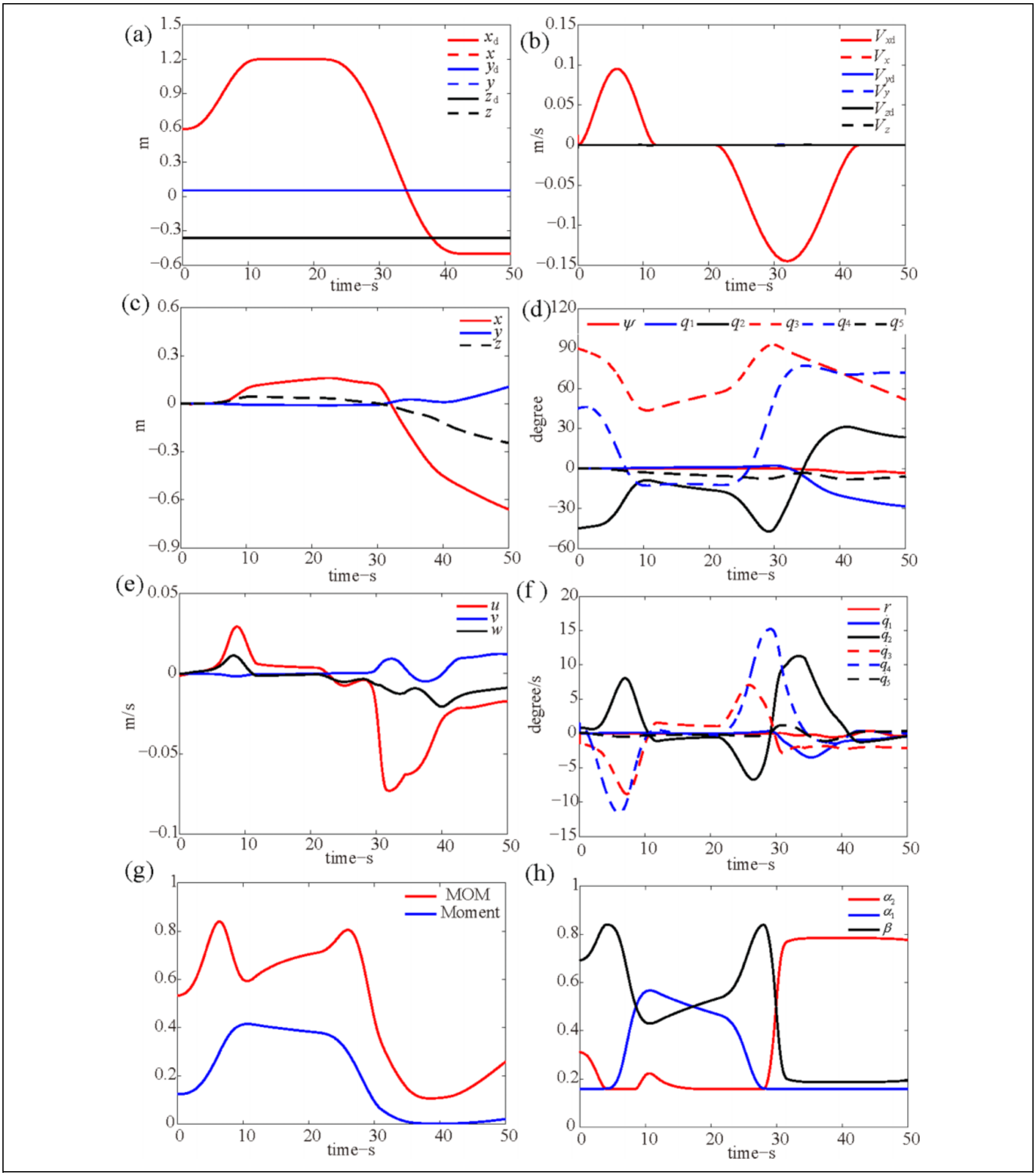

Figure 7. Simulation results under case three. (a) and (b) are the desired trajectory and velocity (solid) versus planned ones (dashed) of the end-effector; (c) and (d) are the planned trajectory for nine DOFs; (e) and (f) are the planned velocity for nine DOFs; (g) is the normalized MOM and moment acting on the underwater vehicle due to *F*; and (h) is the output of the fuzzy algorithm $\alpha_1,\ \alpha_2,\ \beta$. DOF: degree of freedom; MOM: measure of manipulability.

It can be seen from the simulation results of case two that redundancy resolution equation (6) treats the underwater vehicle and manipulator equally without any difference, which, however, is not suitable for practical applications due to the big dynamic difference between the underwater vehicle and manipulator. The underwater vehicle starts to move in the very beginning of the simulation despite the fact that the manipulator is still in its dexterous working space as shown in Figure 5(a) and (c), this may lead to bad control performance. Considering the large mass and low tracking precision of underwater vehicle, this is not good for high-performance tracking control of the end-effector. Furthermore, it can be seen from Figure 5(d) that joint 3 has exceeded the limitation, which clearly shows that redundancy resolution equation (6) has no ability to handle the objective of manipulator joint limitation, which, however, may result in hardware damage.

Comparing the simulation results of case one with case three, it can be clearly observed that our proposed method with the new objective function equations (20) and (21) will limit the movement of the manipulator when the payload is attached as shown in Figure 6(c) and (d). This will greatly reduce the resulting moment and keep the underwater vehicle stable with small pitch and roll angles, which is useful to obtain good control performance since our UVMS has no ability to actively control the pitch and roll angles.

On the other hand, no experimental results had been given in this work limited by practical conditions. But it can be reasonably speculated that our proposed control method may work well in the practical applications. However, some differences compared with the simulation results may appear. Firstly, the trajectories of all signals will become noisy, this is unavoidable due to the existence of measurement noise. Secondly, the vehicle may generate motion all the time. Theoretically, the vehicle should not move when the manipulator is still in its dexterous working space as the simulation results display. In practical situations, the vehicle floats in the water and can be easily disturbed by remaining gravity and external force. Therefore, it will always move since motion controllers are usually based on tracking errors. On the other hand, the motion of vehicle will be suppressed in a certain extent benefiting from our proposed redundancy resolution when the manipulator is in its dexterous working space. Generally speaking, our proposed control method may present some difference with the simulation results, but it will be basically the same.

In conclusion, our proposed redundancy resolution with the new proposed objective function can effectively handle all kinds of secondary objectives and keep the UVMS stable with small pitch and roll angles even under the condition that the manipulator is attached with a large payload, which is very necessary to obtain satisfactory task space tracking control of our UVMS because it has no ability to actively control the pitch and roll angles.

Conclusions

In this article, a new redundancy resolution for UVMS has been proposed and investigated which takes the payload into consideration. Benefiting from the new proposed objective function, the proposed redundancy resolution can effectively keep the UVMS stable with small pitch and roll angles while ensures other secondary objectives. This kind of results is very helpful during the working process. Comparative simulations under three different situations have been conducted, and the corresponding results show that our proposed redundancy can excellently fulfill the task meanwhile ensure a better performance over the traditional method.

Declaration of conflicting interests

The author(s) declared no potential conflicts of interest with respect to the research, authorship, and/or publication of this article.

Funding

The author(s) disclosed receipt of the following financial support for the research, authorship, and/or publication of this article: This work was funded by the National Natural Science Foundation of China (51575283, 51575256) , the Natural Science Foundation of Jiangsu Province (BK20170789), and the Open Foundation of the State Key Laboratory of Fluid Power and Mechatronic Systems (GZKF-201606).

References

1. Ernesto O, Gustavo A, Gerardo J, et al. A passivity-based model-free force–motion control of underwater vehicle–manipulator systems. *IEEE Trans Robot* 2013; 29(6): 1469–1484.
2. Hossein N, Vahid A, and Mohammad D. A time delay controller included terminal sliding mode and fuzzy gain tuning for underwater vehicle–manipulator systems. *Ocean Eng* 2015; 107: 97–107.
3. Ridao P, Carreras M, Ribas D, et al. Intervention AUVs: the next challenge. *Annu Rev Control* 2015; 40: 227–241.
4. Meng W, Yang Q, Jagannathan S, et al. Adaptive neural control of high-order uncertain nonaffine systems: a transformation to affine systems approach. *Automatica* 2014; 50(5): 1473–1480.
5. Wang Y, Gu L, Xu Y, et al. Practical tracking control of robot manipulators with continuous fractional-order nonsingular terminal sliding mode. *IEEE Trans Ind Electron* 2016; 63(10): 6194–6204.
6. Wang Y, Luo G, Gu L, et al. Fractional-order nonsingular terminal sliding mode control of hydraulic manipulators using time delay estimation. *J Vib Control* 2016; 22(19): 3998–4011.
7. Wang Y, Chen J, Gu L, et al. Time delay control of hydraulic manipulators with continuous nonsingular terminal sliding mode. *J Cent South Univ* 2015; 22(19): 4616–4624.
8. Wang Y, Gu L, Gao M, et al. Multivariable output feedback adaptive terminal sliding mode control for underwater vehicles. *Asian J Control* 2016; 18(1): 247–265.
9. Wang Y, Rong S, Chen B, et al. Trajectory tracking control of underwater vehicle–manipulator system using discrete time delay estimation. *IEEE Access* in press; 5: 7435–7443. DOI: 10.1109/ACCESS.2017. 2701350.
10. Meng W, Yang Q, and Sun Y. Guaranteed performance control of DFIG variable-speed wind turbines. *IEEE Trans Control Syst Technol* 2016; 24(6): 2215–2223.

11. Whitney DE. Resolved motion rate control of manipulators and human prostheses. *IEEE Trans Man Mach Syst* 1969; 10(2): 47–53.
12. Liegeois A. Automatic supervisory control of the configuration and behavior of multibody mechanisms. *IEEE Trans Syst Man Cybern* 1977; 7(12): 868–871.
13. Antonelli G and Chiaverini S. Task-priority redundancy resolution for underwater vehicle–manipulator systems In: *Proceedings of the IEEE international conference on robotics and automation*, Leuven, Belgium, 20 May 1998, pp. 768–773. IEEE.
14. Zhao W, Peng S, Wang Y, et al. Fused multiple tasks motion planning for underwater vehicle–manipulator system. In: *Proceedings of the international conference intelligent human–machine systems and cybernetics*, Hangzhou, China, 26–27 August 2013, pp. 322–326. IEEE.
15. Chiaverini S. Singularity-robust task-priority redundancy resolution for real-time kinematic control of robot manipulators. *IEEE Trans Robot Autom* 1997; 13(3): 398–410.
16. Antonelli G and Chiaverini S. A fuzzy approach to redundancy resolution for underwater vehicle–manipulator systems. *Control Eng Pract* 2003; 11(4): 445–452.
17. Antonelli G, Chiaverini S, and Fusco G. A new on-line algorithm for inverse kinematics of robot manipulators ensuring path tracking capability under joint limits. *IEEE Trans Robot Autom* 2003; 19(1): 162–167.
18. Sarkar N and Podder TK. Coordinated motion planning and control of autonomous underwater vehicle–manipulator systems subject to drag optimization. *IEEE J Ocean Eng* 2001; 26(2): 228–239
19. Soylu S, Buckham BJ, and Podhorodeski RP. Redundancy resolution for underwater mobile manipulators. *Ocean Eng* 2010; 37(2–3): 325–343.
20. Ismail ZH and Dunnigan MW. Redundancy resolution for underwater vehicle–manipulator systems with congruent gravity and buoyancy loading optimization. In: *Proceedings of the IEEE international conference on robotics and biomimetics*, Guilin, China, 19–23 December 2009, pp. 1393–1399. IEEE.
21. Zhang Q. *Research on coordinated motion planning and control of autonomous underwater vehicle–manipulator system*. PhD dissertation, Graduate School, Chinese Academy of Sciences, China, 2007.
22. Chan TF and Dubey RV. A weighted least-norm solution based scheme for avoiding joint limits for redundant joint manipulators. *IEEE Trans Robot Autom* 1995; 11(2): 286–292.
23. Yoshikawa T. Manipulability of robotic mechanisms. *Int J Robot Res* 1985; 4(2): 3–9.